

Large-scale drivers of Caucasus climate variability in meteorological records and Mt Elbrus ice cores

Anna Kozachek^{1,2,3}, Vladimir Mikhaleiko², Valérie Masson-Delmotte³, Alexey Ekaykin^{1,4}, Patrick Ginot^{5,6}, Stanislav Kutuzov², Michel Legrand⁵, Vladimir Lipenkov¹, Susanne Preunkert⁵

1. Climate and Environmental Research Laboratory, Arctic and Antarctic Research Institute, Saint Petersburg, 199397, Russia

2. Institute of Geography, Russian Academy of Sciences, Moscow, 119017, Russia

3. Laboratoire des Sciences du Climat et de l'Environnement, CEA/CNRS/UVSQ/IPSL, Gif-sur-Yvette, 91191, France

4. Institute of Earth Sciences, Saint Petersburg State University, Saint Petersburg, 199178, Russia

5. Laboratoire de Glaciologie et Géophysique de l'Environnement, CNRS/UGA, Grenoble, 38400, France

6. Observatoire des Sciences de l'Univers de Grenoble, IRD/UGA/CNRS, Grenoble, 38400, France

Correspondence to: Anna Kozachek (kozachek@aari.ru)

Abstract

A 181.8 m ice core was recovered from a borehole drilled into bedrock on the western plateau of Mt. Elbrus (43°20'53.9'' N, 42°25'36.0'' E; 5115 m a.s.l.) in the Caucasus, Russia, in 2009 (Mikhaleiko et al., 2015). Here, we report on the results of the water stable isotope composition from this ice core in comparison with results from shallow ice cores. There is a distinct seasonal cycle of the isotopic composition which allowed dating by annual layer counting. Dating has been performed for the upper 126 m of the deep core combined with shallow cores data. The whole record covers one century from 2013 back to 1914. Due to the high accumulation rate (1380 mm w.e. per year) and limited melting we obtained the isotopic composition and accumulation rate records with seasonal resolution. These values were compared with available meteorological data from 13 weather stations in the region, and also with atmosphere circulation indices, back-trajectories calculations and GNIP data in order to decipher the drivers of accumulation and ice core isotopic composition in the Caucasus region. In the summer season the isotopic composition depends on the local temperature, while in winter, the atmospheric circulation is the predominant driver of the ice core isotopic composition. The snow accumulation rate correlates well with the precipitation rate in the region all year round, this made it possible to reconstruct and expand the precipitation record at the Caucasus highlands from 1914 till 1966 when the reliable meteorological observations of precipitation at high elevation began.

1 Introduction

Large scale modes of variability such as the NAO (North Atlantic Oscillation) and AMO (Atlantic Multidecadal Oscillation) are known to influence European climate variability (see review in Panagiotopoulos et al., 2002). However, most studies of

large-scale drivers of European climate change have been focused on low elevation instrumental records from weather stations, and there is very limited information about climate variability at high altitudes, and about differences in climate variability and trends at different elevations (EDW research group, 2015). Such differences were calculated in many mountain regions (EDW research group, 2015), except for the Caucasus, due to the lack of high elevation instrumental observations in this region.

The Caucasus is located southwards of the East European Plain. It is a high mountain region, with typical elevations of 3200-3500 m a.s.l., and with the highest point reaching 5642 m for Elbrus. The Main Caucasus Ridge acts as a barrier between subtropical and temperate mid-latitude climates, as observed for other high mountain regions such as the Himalaya. As in other mountain regions, there is a lack of high elevation meteorological records in the Caucasus. Moreover, existing records are relatively short: for example, reliable Caucasus precipitation measurements started only in 1966. An improved spatio-temporal coverage is required to investigate internal variability, to explore trends and spatial differences, and to evaluate the skills of atmospheric models providing atmospheric analysis products where no meteorological data are assimilated.

Measurements of the stable isotope composition of water, and annual accumulation rates in mid to high latitude ice cores are widely used proxies to estimate past temperature and precipitation rate changes. In many high mountain regions such as the Caucasus, and for elevations situated above the tree line, ice core data provides the only source of detailed information to document past climate changes, complementing punctual information retrieved from changes in glacier extent and recent glacier mass balance. For example study of the water stable isotope composition of several ice cores obtained in the Alps was recently conducted by Mariani et al. (2014) and the same research in Alaska was performed by Tsushima et al. (2015). The authors explored the links between the ice cores isotopic composition, local climate and large-scale circulation patterns. They found that in mountain regions isotopic composition of the ice cores governed both by the local meteorological conditions and by the regional and global factors. However, ice core records are complex. For instance, even in areas without any seasonal melt, accumulation is the net effect of precipitation, sublimation, and wind erosion processes, and may significantly differ from precipitation. Water stable isotope records are in mid to high latitudes physically related to condensation temperature through distillation processes, but the climate signal is archived through the snowfall deposition and post-deposition processes. One important artefact lies in the intermittency of precipitation, and the covariance between condensation temperature and precipitation, which may bias the climate record towards one season, or towards one particular weather regime, challenging an interpretation in terms of annual mean temperature. The water isotope content is more sensitive to distortion because of seasonality than the other ice core properties like aerosol concentration (Wagenbach et al., 2012). Moreover, water stable isotopes are integrated tracers of all phase changes occurring from evaporation to mountain condensation, and are also affected by non-local processes related to evaporation characteristics, or shifts in initial moisture sources. Such processes have the potential to alter the validity of an interpretation of the proxy record in terms of local, annual mean, or precipitation-weighted temperature. In some region, isotopic records are more related to hydrological cycles, recycling, rainout (Aemisegger et al., 2014). Finally, the condensation temperature may also strongly differ from surface air temperature, depending on elevation shifts in e.g. planetary boundary layer or convective activity (see Ekaykin

and Lipenkov, 2009 for a review). While these processes make the interpretation of ice core records complex, they conversely open the possibility that the ice core proxy record may be in fact more sensitive to large-scale climate variability than punctual precipitation amounts. For instance, Casado et al (2014) have evidenced a strong fingerprint of the NAO in water stable isotope records from central western Europe and Greenland, either in long instrumental records based on precipitation sampling, in seasonal ice core records, or in atmospheric models including water stable isotopes.

We will now briefly review earlier studies performed on climate variability in the Caucasus area, and which have already explored the relationships between regional climate, glacier expansion, and large-scale modes of variability: the NAO (North Atlantic Oscillation), AO (Arctic Oscillation), AMO (Atlantic Meridional Oscillation) and NCP (North Sea – Caspian Pattern). For example, Shahgedanova et al. (2005) monitored the mass balance of the Djankuat glacier, situated at an altitude between 2700 and 3900 m a.s.l. While no significant correlation was identified between accumulation rate and the winter NAO index, the years of high accumulation systematically occurred during winters with a very negative NAO index. Brunetti et al. (2011) explored the influence of the NCP mode on climate in Europe and around the Mediterranean region. They evidenced a negative correlation coefficient of -0.50 between temperature in the Caucasus and the NCP index. Baldini et al. (2008) investigated records of precipitation isotopic composition in Europe from the IAEA/GNIP stations, extrapolating a significant negative correlation between winter precipitation $\delta^{18}\text{O}$ in the Caucasus region and the NAO index ($R = -0.50$). Casado et al (2013) studied the influence of precipitation intermittency on the relationships between precipitation $\delta^{18}\text{O}$, temperature, and the NAO. The influence of the NAO index on European climate and precipitation $\delta^{18}\text{O}$ appeared more prominent in winter than in summer (Comas-Bru et al., 2016).

Here, we take advantage of the new Elbrus deep ice cores (Mikhalev et al., 2015), and produce the first analysis of water stable isotope and accumulation records. Section 2 introduces the data and methods, with a description of the ice core analyses and age scale, an overview of regional meteorological information, as well as the source of information for indices of modes of variability. Section 3 presents the results of the comparison and statistical analyses of the relationships between regional climate parameters (temperature and precipitation), Elbrus ice core records, and modes of variability. In section 4, we finally summarize our key findings and the next steps envisaged to strengthen the climatic interpretation of the Caucasus ice core records.

2 Data and methods

2.1 Ice core data

2.1.1 Drilling site and drilling campaigns

Here, we report on results from the new, deepest ice core from Mt Elbrus, in comparison with results from shallow ice cores.

104 Deep drilling was performed on the Western Plateau (43°20'53.9" N, 42°25'36.0" E; 5115 m a.s.l.) of Mt Elbrus (fig. 1) in
105 September 2009, allowing recovery of a 181.8 m long ice core, down to bedrock. The drilling site and the drilling operations
106 are thoroughly described in Mikhalevko et al. (2015).

107 In order to update the ice core records towards the present-day, and enable a comparison of the measurements with local
108 meteorological monitoring data, surface drilling operations were repeated at the same place in 2012 (11.5 m long) and in
109 2013 (20.5 m long). Results are also compared here with previously published isotopic composition data measured along the
110 22 m shallow ice core drilled at the same place in 2004 which covered the period from 1998 till 2004. (Mikhalevko et al,
111 2005).

112 In 2014, drilling operations were also successful at the Maili Plateau (Mt. Kazbek), at the altitude of 4500 m a.s.l. in 200 km
113 eastwards from Elbrus (fig. 1), delivering a 20-m ice core. The Kazbek core is shown for the comparison only. Its detailed
114 description will be published elsewhere.

115 116 **2.1.2 Sampling process and sampling resolution**

118 For the upper and the lower parts of the deep core (0-106 m and 158-181.8 m) and for the shallow firn cores drilled in 2012
119 and 2013, sampling was performed using classical cutting-melting procedures. For the other depth intervals, melted samples
120 were extracted from the continuous flow analysis system of LGGE (Grenoble, France), automatically sub-sampled, frozen
121 and stored in vials for subsequent isotopic analysis. The description of the CFA system will be published elsewhere.

122 The sampling resolution was 15 cm for the upper 16 m of the deep core (see the sketch of the sampling resolution in fig. 2c).
123 It was then increased to 5 cm in order to achieve better resolution, from 16 to 70 m depth and in the bottom part of the core
124 (158-182 m depth). To ensure 15-20 samples per year, the sampling resolution was increased to 4 cm in the depth range from
125 70 to 106 m, similar to the sampling resolution of the CFA system (3.7 cm).

126 Samples from the shallow cores drilled in 2012 and 2013 were cut with a resolution of 10 and 5 cm, respectively.

127 128 **2.1.3 Isotopic measurements**

130 Water stable isotope ratios ($\delta^{18}\text{O}$ and δD) were measured at the Climate and Environmental Research Laboratory (CERL) of
131 Arctic and Antarctic research Institute (St Petersburg, Russia), using a Picarro L2120-i analyzer. Each sample was measured
132 once. Sequences of measurements included the injection of 5 samples, followed by the injection of an internal laboratory
133 standard with an isotopic value close to that of the samples. We also repeated the measurements of about 10% of all the
134 samples in order to calculate the analytical precision: 0.06‰ for $\delta^{18}\text{O}$ and 0.30‰ for δD . The depth profile of $\delta^{18}\text{O}$
135 (Mikhalevko et al., 2015; Kozachek et al., 2015) and of the deuterium excess ($d = \delta\text{D} - 8 \cdot \delta^{18}\text{O}$) are shown in fig. 2.

136 Moreover, 600 samples from the depth interval from 23 to 35 m were measured in the Laboratory of Isotope Hydrology of
137 the IAEA (Vienna, Austria). The two records are highly correlated ($r=0.99$, $p < 0.05$) for both isotopes (Figure S2b) with a

138 systematic offset of 0.2 ‰ for $\delta^{18}\text{O}$ and 1 ‰ for δD . The records of the second order parameter deuterium excess are also
139 significantly correlated ($r=0.65$, $p < 0.05$) without any specific trend or systematic offset. This inter-laboratory comparison
140 demonstrates the high quality of the isotopic measurements performed in CERL.

141 We also stress the close overlap of the upper part of the profiles of the water stable isotope records versus depth from the
142 different cores drilled in 2009, 2012 and 2013 (Fig. S2a). Based on this close agreement within the different shallow firn
143 cores, we decided to calculate a stack record for the period from 1914 till 2013 which is used hereafter for the dating.

144 In the depth interval from 100 to 106 m depth, we also have an overlap of samples obtained with classical cutting method
145 and CFA method described above, without any significant difference (Fig. S2c), again allowing us to combine the two
146 records into one stack record.

147

148 **2.1.4 Dating**

149

150 The chronology is based on the identification of annual layers. These are prominent in $\delta^{18}\text{O}$ with the average seasonal
151 amplitude of 20 ‰. We used the mean value of the $\delta^{18}\text{O}$ of the whole dataset (-15.5 ‰) as a threshold to separate between
152 the warm and cold seasons. For equivocal situations, we also used additional data: melt layers and dust layers (used to
153 identify the warm season) (Kutuzov et al., 2013) as well as ammonium and succinic acid concentration data that also have
154 seasonal variations (Mikhalenko et al., 2015). We compared annual layers counting performed independently using the
155 seasonal cycles in the isotopic composition and the ammonium concentration. The discrepancy between two independent
156 chronologies is ± 1 year at a depth of 126 m. Hereafter, we focus our analysis on one century, from 1914 till 2013, which
157 corresponds to the upper 126 m of the core. This period has been chosen because of relatively small dating uncertainty (± 1
158 year) and the availability of other records such as local meteorological observations. Figure 3 illustrates the identification of
159 years. For a detailed description of the raw isotopic data and annual layers allocation for the upper 106 m of the core, please
160 refer to Mikhalenko et al. (2015). Mean seasonal values of $\delta^{18}\text{O}$ and d obtained as a result of the dating are shown in fig. 5
161 and 6 respectively.

162 The annual accumulation rate is calculated as the thickness of the seasonal layer, multiplied by the layer density using the
163 density profile from Mikhalenko et al. (2015), and corrected for layer thinning using the Dansgaard-Johnsen model
164 (Dansgaard and Johnsen, 1969), with the following parameters: accumulation rate 1.583 m of ice equivalent, pore close-off
165 depth = 55 m (Mikhalenko et al., 2015).

166

167 **2.1.5 Diffusion of stable isotopes**

168

169 We calculated the potential influence of diffusion on the stable isotopes record according to (Johnsen, 2000) model. Our
170 calculation showed that the seasonal amplitude of $\delta^{18}\text{O}$ variations could be 10-20% less because of the diffusion. If it was the
171 case we would observe a decreasing of $\delta^{18}\text{O}$ maxima and increasing of minima with depth. Moreover we would find a

172 positive correlation between accumulation rate and seasonal amplitude of $\delta^{18}\text{O}$. These features have not been found in the ice
173 core data. We therefore consider that the diffusion does not influence sufficiently the isotopic composition record in the
174 upper 126 m of the ice core. At the bottom part of the core (e.g. at a depth of 180 m) the annual cycle of $\delta^{18}\text{O}$ should have an
175 amplitude of 4 ‰ which is detectable but the length of the cycle should be less than 1 cm. Thus, for obtaining climatic
176 information from the bottom part of the core very high sampling resolution is required.

177 178 **2.2 Meteorological data**

179
180 We used the daily meteorological data (precipitation rate and mean daily temperature) from several weather stations around
181 the drilling site (see map in Fig. 1 and Table 1) for comparison with the ice core data. We also investigated records of
182 precipitation isotopic composition based on monthly sampling, performed at three stations to the south of Caucasus within
183 the WMO-IAEA Global Network of Isotopes in Precipitation (GNIP) program (Table 1).
184 For comparison we used the NCEP/NCAR reanalysis temperature data (Kalnay et al., 1996) for the 500 mbar level which
185 corresponds to the drilling site altitude. Two different models were used to calculate back trajectories: FLEXPART (Forster
186 et al., 2007, Stohl et al., 2009), HYSPLIT (Draxler, 1999, Stein et al., 2015, Rolph, 2016). The LMDZiso model was used to
187 estimate the precipitation isotopic composition at the drilling site (Risi et al., 2010).

188 189 **3 Results**

190 191 **3.1 Regional climate**

192
193 The main peculiarity of the drilling site is its location on the border between subtropical and temperate climatic zones
194 (Volodicheva, 2004). Back-trajectory calculations show that the drilling site is characterized by remarkable seasonal
195 differences in moisture sources locations. In winter, the origin of air masses varies from the Mediterranean to the North
196 Atlantic. In summer, local moisture sources from the surrounding continents or from the Black Sea are predominant (see fig.
197 S1 for examples).

198 Meteorological data depict large regional variations in the seasonal cycle of precipitation. To the south of the Caucasus, there
199 is no distinct seasonal cycle (Fig. 4a), showing the climatology for the Klukhorsky Pereval station. In fact, the Klukhorsky
200 Pereval station is situated north of the Main ridge, but in terms of the seasonal cycle of precipitation it undoubtedly belongs
201 to the southern group. But we are nevertheless using this station as an example because of the uninterrupted record of
202 temperature and precipitation for the 1966-1990 period. By contrast, the north of the Caucasus is marked by a distinct
203 seasonality in precipitation amounts, which are maximum in summer and minimum in winter (Fig. 4b), showing the
204 climatology for the Mineralnye Vody station. Moreover, the annual precipitation rate to the south of the Caucasus is much
205 higher than to the north. For example, the typical annual precipitation rate to the north of the Caucasus at the altitude close to

the sea level is 500 mm per year, while to the south of the Caucasus at the same altitude it is about 1500 mm. The amount of precipitation in the region is affected by the altitude and the distance from the sea shore.

The seasonal changes of temperature appear uniform all over the region surrounding Caucasus, with warmest conditions observed in summer and coldest conditions observed in winter. The seasonal amplitude depends on the distance from the sea and the mean annual temperature depends on the altitude. The average regional lapse rate was calculated using the available meteorological data. It is minimum in winter (2.3°C per 1000 m) and maximum (5.2 °C per 1000 m) in summer (Fig. S3).

Based on the coherency of temperature variability at all the weather stations in this region, we calculated a regional stack temperature record. Normalized temperature time series were calculated for each station for each season or for the whole year, and results were then averaged (see Fig. 8a and 8b for seasonal stack records). For precipitation data, available in this region since 1966, we considered two different stacks (fig. S4), separating the stations with a distinct seasonal cycle from those where no seasonal cycle was identified for precipitation rates. We coherently used the reference period from 1966 to 1990 for normalization for both precipitation rate and temperature.

At our drilling site, an automatic weather station (AWS) provided in situ measurements for the period from August 2007 till January 2008. The day to day variations of temperature at low elevation weather stations and at the AWS are coherent for the whole period of the AWS work.

We also compared the data from meteorological stations with the NCEP reanalysis (Kalnay et al., 1996) outputs (not shown) for the 500 mbar level. Despite difference in absolute values on the daily scale when compared with the AWS data (the difference is random and varies from -1 to 1 °C), the observed regional data and reanalysis data have the same month to month variability. The maximum daily mean temperature at the drilling site according to the reanalysis data was -1.3 °C for the whole dataset. The temperature in the glacier at 10m depth, which correspond to the annual mean temperature at the drilling altitude, is -17 °C (Mikhaleenko et al., 2015), the annual mean temperature at the drilling altitude from the NCEP reanalysis is -14 °C, and the same value calculated from meteorological observations and corrected for the lapse rate is -11 °C.

Hereafter in the meteorological data, we considered the cold season or winter of a given year to range from November of the previous year till April of the current year, and the warm season or summer from May till October.

We then investigated long-term trends in the composite meteorological records. It is evident that last 20 years in summer season were the warmest for the whole observation period (fig. 8), while in winter the recent warming is not unprecedented. For example, winters in the 1960s – 1970s were even warmer (fig. 8). Multi-decadal patterns of temperature variations also differ in the late 19th Century, where negative anomalies are identified in winter temperature (Fig. 8) but not in summer temperature (Fig 8). On the other hand in winter temperatures we can observe lower temperatures at the end of 19th century that can be impact of the volcanic eruptions (Stoffel et al., 2015). We also noted the high temperature values in the 1910s - 1920s that is not completely understood. We did not find any trends in the precipitation rate for neither of the groups of stations (fig. S4).

A significant anti-correlation is observed between temperature and the NAO index, both in winter and summer (Table 2, the information about the time series used for the correlation analysis can be found in Table 1). Stronger anti-correlations are identified between temperature and the NCP index, especially in winter, as also reported by Brunetti et al. (2011). A weak positive correlation is identified between AMO and summer temperature. Relationships with indices of large scale modes of variability are systematically weaker for precipitation, with contradictory results for the south\north Caucasus stack; they appear significant for the NCP in summer and winter (Table 2).

GNIP data are only available at low elevation stations. They show a rather uniform distribution of the isotopic composition of precipitation in the region during summer, as well as a gradual depletion of $\delta^{18}\text{O}$ at higher altitudes in winter.

GNIP records are too short and intermittent (one-two years with gaps) to investigate the variability and relationships with the local temperature on interannual scale. We therefore restrict discussion of GNIP data to seasonal variations. The $\delta^{18}\text{O}$ and δD in precipitation have a distinct seasonal cycle with maximum values observed in warm season (JJA) and minimum values observed in cold season (DJF). As an example we show the seasonal cycle of $\delta^{18}\text{O}$ and d for Bakuriani station in 2009 (fig. 7). This station is the only one in the region for which the whole uninterrupted dataset for one annual cycle is available. The seasonal amplitude of $\delta^{18}\text{O}$ is about 10 ‰. The d variations show no seasonal cycle varying randomly between 10 ‰ and 25 ‰. We found no significant correlation between $\delta^{18}\text{O}$ and d .

Climate variability as a driver for glacier variations in the Caucasus has recently been explored by several authors. Elizbarashvili et al. (2013) found the increased frequency of extremely hot months during the 20th century, especially over Eastern Georgia, whereas number of extremely cold months decreased faster in the Eastern than in the Western region. In addition, highest rates for positive trends of annual mean air temperature can be observed in the Caucasus Mountains. Shahgedanova et al. (2014) evidenced significant glacier recession at the northern slopes of the Caucasus, consistent with increasing air temperature of the ablation season. They report that the most recent decade (2001-2010) was 0.7 – 0.8 °C warmer than in 1960-1986 at Terskol and Klukhorskiy Pereval stations (see Table 1 for information on stations). However, the warmest decade for JJA was 1951-1960 (Shahgedanova et al., 2014). Tielidze (2016) reports recent increase of the annual mean temperatures at different elevations in the Georgian Caucasus. The region experienced glacier area loss over the 20th century at an average annual rate of 0.4% with a higher rate in eastern Caucasus than in the central and western sections. The analysis of temperature and radiation regime of glaciers at the ablation period has been performed at Elbrus vicinities recently (Toropov et al., 2016). The authors prove that the observed waning of glaciers can not be explained by increase of temperature during the ablation period because of increase of precipitation during the accumulation period. They concluded that the main driver of glacier retreat is increase of the solar radiation balance for 4% for the 2001-2010 period which corresponds to increase of ablation for 140 mm per ablation season (Toropov et al., 2016).

3.2 Ice core records

272 The comparison of the four cores obtained at the Western Plateau of Elbrus shows similar variations during overlap periods
 273 (see Fig. 2S). We therefore calculate a stack record for each season, based on the average value of individual ice cores for the
 274 overlapping seasons. The inter-core disagreement is almost negligible (fig. 2S) and can be explained by different sampling
 275 resolution.

276 We note that the shallow ice core from the Maili plateau of Kazbek shows the same mean values of $\delta^{18}\text{O}$ as the Elbrus ice
 277 cores during their overlap period. This is a surprise, given the difference in elevation (500 m) and continentality (200 km
 278 distance).

279 The inter-annual variability in isotopic composition is about twice larger in winter than in summer for $\delta^{18}\text{O}$. Different
 280 patterns of inter-annual to multi-decadal variations appear in the instrumental temperature data (see section 3.1) and ice core
 281 $\delta^{18}\text{O}$ records (Fig 5) emerge for winter versus summer. Consequently, we do not investigate annual mean results, and focus
 282 on each season.

283 The δD and $\delta^{18}\text{O}$ values are highly correlated ($r = 0.99$) on sample to sample scale so hereafter we use the $\delta^{18}\text{O}$ information
 284 for the dating and comparison with the other parameters. The slope between $\delta^{18}\text{O}$ and δD is 8.03 on sample to sample scale
 285 and 7.9 on seasonal scale without any significant difference between the two seasons.

286 No significant (R squared is insignificant at $p < 0.05$) centennial trend is identified in winter / summer $\delta^{18}\text{O}$, nor in winter /
 287 summer accumulation rate or deuterium excess. We observe large variations in $\delta^{18}\text{O}$ with high and variable values early 20th
 288 century, lower and more stable values in the 1940s-1960s, and a step increase in the 1970s with another level. These
 289 variations are coherent in both seasons but are not reflected in the meteorological observations. There is also an increase of
 290 $\delta^{18}\text{O}$ in the last two decades in both seasons in regard to the 1970s-1980s values but the absolute values of $\delta^{18}\text{O}$ are close to
 291 the multiannual seasonal averages (Table 3). The highest decadal values of $\delta^{18}\text{O}$ in both summer and winter are observed in
 292 1912-1920. While a recent warming trend is observed in the regional meteorological data (in summer), it is much less
 293 prominent in the ice core $\delta^{18}\text{O}$ record, suggesting a divergence between $\delta^{18}\text{O}$ and regional temperature. One of the possible
 294 explanations for this feature is the post-depositional change of the isotopic composition. But we do not expect a significant
 295 influence of the post-depositional processes because of high snow accumulation rate. The highest $\delta^{18}\text{O}$ values for a single
 296 year correspond to the summer periods of 1984 and 1928, two years for which no unusual feature is identified from
 297 meteorological observations. The highest snow accumulation rate (fig. 9) is observed in both seasons of 2010, in coherence
 298 with the meteorological precipitation data, and also corresponding with a record low winter NAO index.

299 Our deuterium excess record (fig. 2b) does not depict any robust seasonal variation. Moreover, the distribution of deuterium
 300 excess as a function of $\delta^{18}\text{O}$ does not display any clear structure. By contrast, deuterium excess is weakly positively
 301 correlated with the accumulation rate during summer ($r = 0.27$, $p < 0.05$). This finding is consistent with the GNIP data in the
 302 region that show no link between $\delta^{18}\text{O}$ and deuterium excess. The smoothed values of deuterium excess have prominent
 303 cycles with a period of about 25 years that are synchronous in both seasons (fig. 6). Deuterium excess is highly sensitive to
 304 surface humidity, which itself is very different and depends on the arrival of maritime air masses or dry continental air
 305 masses. This may add to the complexity of the deuterium excess signal (Pfahl and Wernli, 2008).

3.3 Comparison of ice core records with regional meteorological data

We compared the ice core data with the regional meteorological data and the large scale modes of variability. The result of the correlation analysis is summarized in Table 4. Multiannual variations of the parameters are shown in fig. 9 for the winter period and in fig. 10 for the summer period.

We found no significant correlation between the ice core $\delta^{18}\text{O}$ record and regional temperature, neither with the reanalysis data, nor with the observation data, when using the whole period. A significant correlation ($r = 0.52$, $p < 0.05$) emerges for summer data, when calculated for the period since 1984. The slope for this period is 0.25 per mille per $^{\circ}\text{C}$. We also repeated our linear correlation analysis using precipitation weighted temperature, and obtained the same results. This result implies that the isotopic composition at Elbrus is controlled by both local and regional factors such as changes in moisture sources. The possibilities for accurate reconstructions of past temperatures are therefore limited. For more accurate investigation of the $\delta^{18}\text{O}$ – temperature relation on-site experiments and subsequent modelling is required. Our results are comparable to those obtained in the Alps by Mariani et al. (2014): again, while the seasonal cycle of ice core $\delta^{18}\text{O}$ appears related to that of temperature, this is not the case for inter-annual variations, driven by other factors such as changes in moisture sources. Another research performed in the Alps by (Bohleber et al., 2013) revealed significant correlation of modified local temperature and the ice core isotopic composition at decadal scale. The authors also report that there are some periods of correlation absence. The main finding is that for the periods of less than 25 years the difference between the modified according to the authors' method and original dataset temperature is crucial but for longer periods the two temperature datasets are close to each other. That conclusion implies that the isotopic composition reflects the local temperature in the high mountain regions to a limited extent. It seems to be impossible to calculate the modified temperature for the Caucasus region according to the methods described by (Bohleber et al., 2013) because of the relatively short and sparse original datasets.

We also compared the annual mean temperatures and $\delta^{18}\text{O}$ values disregarding the difference in the isotopic composition trends in different seasons. The regression analysis showed significant negative correlation between the two parameters. The regression equation for 11-year running means in the 1914-1928 and 1994-2013 differs from the same for the 1929-1993 (see fig. 11 for the correlation plot and regression equations). The shifts can be explained by a sharp change of the climatic system. The negative correlation between $\delta^{18}\text{O}$ and local temperature has already been observed in Antarctica (Vladimirova and Ekaykin, 2014). It can be explained by the change of the moisture source that can lead to increase of the difference between the source temperature and local temperature while local temperature slightly decreases.

Seasonal accumulation rate is linked to the precipitation rate on the stations situated south of the Caucasus in both seasons ($r = 0.45$), and even more closely related to precipitation from Klukhorski Pereval station ($r = 0.65$ for both seasons). We therefore establish a linear regression model for the period 1966-2013, and use this methodology to reconstruct past precipitation rates (1914-1965), when meteorological records are not reliable or not available. The reconstructed records are

shown on fig. 9 and 10 for the winter and summer seasons respectively. We found no significant trend in the reconstructed precipitation values. Even so, these results can be useful for validation of regional climate models and water resource assesment.

Calculation of the seasonal cycle of precipitation isotopic composition using the LMDZiso model (Risi et al., 2010) do not correspond to the results obtained from the ice core in absolute values or in amplitude. This can be explained by a complicated relief of the region that influences strongly the isotopic composition, but it is not taken into account in the model. Also in summer Elbrus is in a local convective precipitation system that is not included in the model.

3.4 Comparison of ice core records with large scale modes of variability

We report a significant ($p < 0.05$) negative correlation ($r = -0.33$) between the ice core accumulation rate record and NAO in winter. Moreover, the year of extremely high accumulation in both seasons (2010) coincides with an extremely low NAO winter index. The role of NAO in regional climate had also been evidenced by Shahgedanova et al. (2005) for the mass-balance of the Djankuat glacier situated in 30 km south-east of Elbrus for the period of 1967-2001. Interestingly, the accumulation record is related to the variability of regional precipitation, but the latter is not significantly related to the NAO. This may suggest different influences of large-scale atmospheric circulation on precipitation at lower versus higher elevations.

The ice core winter $\delta^{18}\text{O}$ record shows a positive correlation with the NAO index ($r = 0.42$), while the NAO index is negatively correlated with regional temperature ($r = -0.42$). It also contradicts the findings of Baldini et al (2008) who, based on the GNIP low elevation dataset, extrapolated a negative correlation between the $\delta^{18}\text{O}$ of precipitation and the NAO in this region. This finding also suggests different drivers of temperature and $\delta^{18}\text{O}$ at low and higher elevation. We propose the following explanation for this correlation. During the positive NAO phase, the predominant moisture source for the Caucasus precipitation is the Mediterranean. During the negative NAO phase the moisture source is the Atlantic. In the first case the precipitation $\delta^{18}\text{O}$ preserved in the ice core is higher because of higher initial sea water isotopic composition (Gat et al., 1996) and shorter distillation pathway. In the opposite situation the initial water isotopic composition is close to 0 ‰ (Frew et al., 2000) and the distillation pathway is longer which leads to lower values of precipitation $\delta^{18}\text{O}$.

In order to explore the relationships of the Elbrus ice core datasets with the AMO, we used 20-year smoothed data. We show a negative correlation between the AMO index and the summer ice core $\delta^{18}\text{O}$ signal ($r = -0.53$) and a positive correlation between the AMO index and the winter accumulation record ($r = 0.52$). As the correlation analysis between the ice core data and AMO index was performed with smoothed records it is not reported in Table 4, in order to avoid misunderstanding.

We explored the links between the ice core parameters ($\delta^{18}\text{O}$, accumulation rate) with the NCP index and found no significant correlation neither in winter nor in summer despite the significant correlation between the NCP and local temperature and precipitation. A possible explanation may be that the NCP pattern only affects low elevation regional climate but not high elevation climate.

No significant correlation was identified between deuterium excess and indices of large scale modes of variability. So far, no regional or large-scale climate signal could be identified in Elbrus deuterium excess. Further investigations using backtrajectories and diagnoses of moisture source and evaporation characteristics will be needed to explore further the drivers of this second-order isotopic parameter.

4 Conclusion

We found no persistent link between ice cores $\delta^{18}\text{O}$ and temperature, common feature emerging from non-polar ice cores (e.g. Mariani et al., 2014). This finding is not an artifact of high elevation versus low elevation difference because the variability of the regional temperature stack used for this comparison is in good agreement with the variability of the temperature at the drilling site as observed by the local AWS.

Our ice core records depict large decadal variations in $\delta^{18}\text{O}$ with high and variable values in the late 19th - early 20th centuries, lower and more stable values in the 1940s-1960s, followed by a step increase in the 1970s. No unusual recent change is detected in the isotopic composition or in the accumulation rate record, in contrast with the observed warming trend from regional meteorological data. The accumulation rate appears significantly related to the NAO index coherently with the earlier results for the Djankuat glacier (Shahgedanova et al. 2005).

Based on regional meteorological information and trajectory analyses, the main moisture source is situated not far from the drilling site in summer, and consists of evaporation from the Black Sea and continental evapotranspiration. Changes in regional temperature during summer may affect the initial vapour isotopic composition as well as the atmospheric distillation processes, including convective activity, in a complex way. This may explain the significant albeit non persistent correlation of summer $\delta^{18}\text{O}$ and temperature. Winter moisture sources appear more variable geographically, with potential contributions from the North Atlantic to the Mediterranean regions. Changes in moisture origin appear to dominate in regional temperature-driven distillation processes. As a result, the ice core isotopic composition appears mostly related to characteristics of large –scale atmosphere circulation such as the NAO index. The changes in moisture origin also influence deuterium excess parameter, which does not have any prominent seasonal variations.

Our data can be used in atmospheric models equipped with water stable isotopes for instance in order to assess their ability to resolve NAO – water isotope relationships (Langebroek et al., 2011, Casado et al., 2014). The accumulation rate at the drilling site is highly correlated with the precipitation rate and gives information about precipitation variability before the beginning of meteorological observations.

Acknowledgements

The research was supported by the RFBR grant 14-05-31102, the measurement of the samples in IAEA was conducted according to research contracts 16184\R0, and 16795. This research work was conducted in the framework of the

International Associated Laboratory (LIA) “Climate and Environments from Ice Archives” 2012–2016, linking several Russian and French laboratories and institutes. We thank Obbe Tuinenburg and Jean-Louis Bonne for the back trajectories calculations.

References

- Aemisegger F., Pfahl S., Sodemann H., Lehner I., Seneviratne S.I., Wernli H.: Deuterium excess as a proxy for continental moisture recycling and plant transpiration, *Atmos. Chem. Phys*, 14, 4029–4054, doi:10.5194/acp-14-4029-2014, 2014.
- Baldini L.M., McDermott F., Foley A.M., Baldini J.U.L.: Spatial variability in the European winter precipitation $\delta^{18}\text{O}$ -NAO relationship: Implications for reconstructing NAO-mode climate variability in the Holocene, *Geophys. Res. Letters*, 35, doi:10.1029/2007GL032027, L04709, 2008.
- Bohleber P., Wagenbach D., Schoner W., Bohm R.: To what extent do water isotope record from low accumulation Alpine ice cores reproduce instrumental temperature series? *Tellus B*, 65, 20148, doi:10.3402/tellusb.v65i0.20148, 2013.
- Brunetti M., Kutiel H.: The relevance of the North-Sea Caspian Pattern (NCP) in explaining temperature variability in Europe and the Mediterranean, *Nat. Hazards Earth Syst. Sci.*, 11, 2881–2888, doi:10.5194/nhess-11-2881-2011, 2011.
- Casado M, Ortega P., Masson-Delmotte V., Risi C., Swingedouw D., Daux V., Genty D., Maignan F., Solomina O., Vinter B., Viovy N., Yiou P.: Impact of precipitation intermittency on NAO-temperature records, *Clim. Past*, 9, 871–886, doi:10.5194/cp-9-871-2013, 2013.
- Comas-Bru, L., McDermott, F. and Werner, M. (2016): The effect of the East Atlantic pattern on the precipitation $\delta^{18}\text{O}$ -NAO relationship in Europe, *Climate Dynamics*, doi: 10.1007/s00382-015-2950-1
- Dansgaard, W., Johnsen, S.J.: A flow model and a time scale for the ice core from Camp Century, Greenland, *J. Glaciol.*, 8(53), 215–223, 1969.
- Draxler, R.R., and Hess G.D.: An overview of the HYSPLIT_4 modeling system of trajectories, dispersion, and deposition. *Aust. Meteor. Mag.*, 47, 295–308, 1998.
- Ekaykin A.A., Lipenkov V.Ya.: Formation of the ice core isotopic composition, *Physics of ice core records II*, ed. T.Hondoh, *Low Temperature Science*, 68, Hokkaido Univ. Press, Sapporo, 299–314, 2009.
- Elizbarashvili E.Sh., Elizbarashvili, M.R., Tatishvili, M.E., Elizbarashvili, Sh.E., Elizbarashvili, R.Sh.: Meskhiya Air temperature trends in Georgia under global warming conditions, *Russ. Meteorol. Hydrol.*, 38, 234–238, 2013.
- Forster C., Stohl A., Siebert P.: Parametrization of convective transport in a lagrangian particle dispersion model and its evaluation, *Journ. of Applied Meteorology and Climatology*, 46 (4), 403–422, doi:10.1175/JAM2470.1, 2007.
- Frew, R., Dennis, P.F., Heywood K.J., Meredith M.P., and Boswell S.M.: The oxygen isotope composition of water masses in the northern North Atlantic, *Deep Sea Research Part I: Oceanographic Research Papers*, 47, 12, 2265–2286, doi:10.1016/S0967-0637(00)00023-6, 2000.
- Gat, J.R., Shemesh, A., Tziperman, E., Hecht, A., Georgopoulos, D., and Basturk, O.: The stable isotope composition of waters of the eastern Mediterranean Sea, *J. Geophysical Res.*, 101, 3, 6441–6451, doi: 10.1029/95JC02829, 1996.

Johnsen S., Clausen H.B., Cuffey K.M., Hoffmann G., Schwander J., Creyts T.: Diffusion of stable isotopes in polar firn and ice: the isotope effect in firn diffusion, *Physics of Ice Core Records*, Edited by T. Hondoh, Hokkaido University Press, Sapporo, 121–140, 2000.

Kalnay, E., Kanamitsu, M., Kistler, R., Collins, W., Deaven, D., Gandin, L., Iredell, M., Saha, S., White, G., Woollen, J., Zhu, Y., Leetmaa, A., Reynolds, B., Chelliah, M., Ebisuzaki, W., Higgins, W., Janowiak, J., Mo, K. C., Ropelewski, C., Wang, J., Jenne, R., Joseph, D.: The NCEP/NCAR 40-Year Reanalysis Project, *Bulletin of the American Meteorological Society*, 77, 3, 437–472, doi: 10.1175/1520-0477(1996)077<0437:TNYRP>2.0.CO;2, 1996.

Kozachek A.V., Ekaykin A.A., Mikhaleiko V.N., Lipenkov V.Y., Kutuzov S.S.: Isotopic composition of ice cores obtained at the Elbrus Western Plateau, *Ice and Snow*, 55, 4, doi: 10.15356/2076-6734-2015-4-35-49, 35–49, 2015 (in Russian with English summary)

Kutuzov, S., Shahgedanova, M., Mikhaleiko, V., Lavrentiev, I., and Kemp, S.: Desert dust deposition on Mt. Elbrus, Caucasus Mountains, Russia in 2009–2012 as recorded in snow and shallow ice core: high-resolution “provenancing”, transport patterns, physical properties and soluble ionic composition, *The Cryosphere*, 7(5), 1481–1498, doi:10.5194/tc-7-1481-2013, 2013.

Langebroek, P. M.; Werner, M.; Lohmann, G.: Climate information imprinted in oxygen-isotopic composition of precipitation in Europe, *Earth and Planetary Science Letters*, 311, 1, 144–154, 10.1016/j.epsl.2011.08.049, 2011.

Mariani I., Eichler A., Jenk M., Brönnimann S., Auchmann R., Leuenberger M.C., Schwikowski M.: Temperature and precipitation signal in two Alpine ice cores over the period 1961–2001, *Clim. Past*. 10, 1093–1108, doi:10.5194/cp-10-1093-2014, 2014.

Mikhaleiko V., Sokratov S., Kutuzov S., Ginot P., Legrand M., Preunkert S., Lavrentiev I., Kozachek A., Ekaykin A., Faïn X., Lim S., Schotterer U., Lipenkov V., Toropov P.: Investigation of a deep ice core from the Elbrus western plateau, the Caucasus, Russia, *The Cryosphere*, 9, 2253–2270, doi:10.5194/tc-9-2253-2015, 2015.

Mikhaleiko, V.N., Kuruzov, S.S., Lavrentiev, I.I., Kunakhovich, M.G., and Thompson, L.G.: Issledovanie zapadnogo lednikovogo plato Elbrusa: rezul'taty i perspektivy (Western Elbrus Plateau studies: results and perspectives), *Materialy glyatsiologicheskikh issledovaniy (Data Glaciol. Stud.)*, (99), 185–190, 2005 (in Russian with English summary)

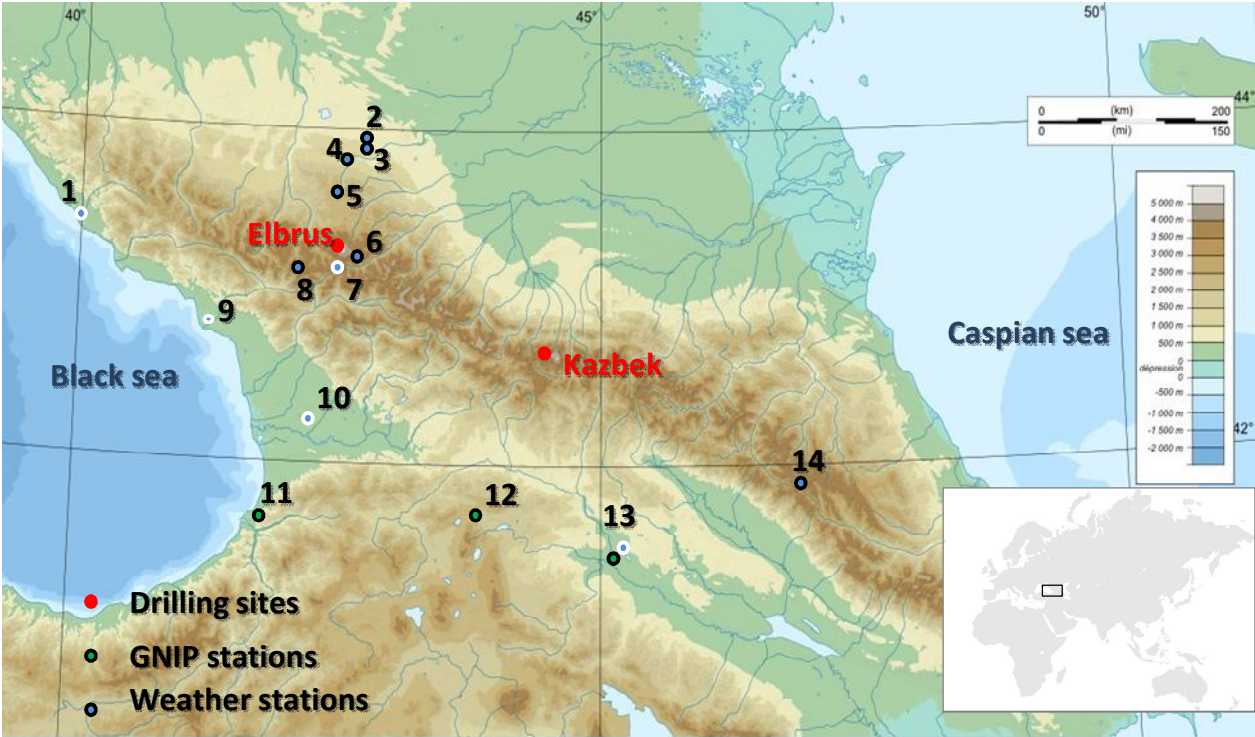
Mountain Research Initiative EDW Working Group: Elevation-dependent warming in mountain regions of the world, *Nature Climate Change* 5, 424–430, doi:10.1038/nclimate2563, 2015.

Panagiotopoulos F., Shahgedanova M., Steffenson D.B.: A review of Northern Hemisphere winter time teleconnection patterns, *J. Phys. IV France*, 12, doi: 10.1051/jp4:20020450, 2002.

Pfahl S. and Wernli H.: Air parcel trajectory analysis of stable isotopes in water vapor in the eastern Mediterranean, *J. Geophys. Res.*, 113, D20104, doi:10.1029/2008JD009839, 2008.

Risi C., Bony S., Vimeux F., Jouzel J.: Water stable isotopes in the LMDZ4 general circulation model: Model evaluation for present-day and past climate and implications to climatic interpretation of tropical isotopic records, *Journal of Geophysical Research*, 115, D12118, doi:10.1029/2009JD013255, 2010.

476 Rolph, G.D., Real-time Environmental Applications and Display sYstem (READY) Website (<http://ready.arl.noaa.gov>).
 477 NOAA Air Resources Laboratory, Silver Spring, MD, 2016.
 478 Shahgedanova M., Nosenko G., Kutuzov S., Rototaeva O., and Khromova T.: Deglaciation of the Caucasus Mountains,
 479 Russia/Georgia, in the 21st century observed with ASTER satellite imagery and aerial photography, *The Cryosphere*, 8(6),
 480 2367–2379, doi:10.5194/tc-8-2367-2014, 2014.
 481 Shahgedanova M., Stokes C., Gurney S., Popovnin V.: Interactions between mass balance, atmospheric circulation, and
 482 recent climate change on the Djankuat Glacier, Caucasus Mountains, Russia, *Journ. of Geophys. Research*, 110, D04108,
 483 doi:10.1029/2004JD005213, 2005.
 484 Stein, A.F., Draxler, R.R., Rolph, G.D., Stunder, B.J.B., Cohen, M.D., and Ngan, F.: NOAA's HYSPLIT atmospheric
 485 transport and dispersion modeling system, *Bull. Amer. Meteor. Soc.*, 96, 2059–2077, doi: 10.1175/BAMS-D-14-00110.1,
 486 2015.
 487 Stoffel M., Khodri M., Corona C., Guillet S., Poulain V., Bekki S., Guiot J., Luckman B.H., Oppenheimer C., Lebas N.,
 488 Beniston M., and Masson-Delmotte V.: Estimates of volcanic-induced cooling in the Northern Hemisphere over the past
 489 1,500 years, *Nature Geoscience* 8, 784–788, doi:10.1038/ngeo2526, 2015.
 490 Stohl A., Thompson D.J.: A density correction for lagrangian particle dispersion models, *Boundary Layer Meteorology*, 90
 491 (1), 155–167, doi:10.1023/A:1001741110696, 1999.
 492 Tielidze L.G.: Glacier change over the last century, Caucasus Mountains, Georgia, observed from old topographical maps,
 493 Landsat and ASTER satellite imagery, *The Cryosphere*, 10, 713–725, doi:10.5194/tc-10-713-2016, 2016.
 494 Toropov P.A., Mikhaleiko V.N., Kutuzov S.S., Morozova P.A., Shestakova A.A.: Temperature and radiation regime of
 495 glaciers on slopes of the Mount Elbrus in the ablation period over last 65 years, *Ice and Snow*, 56(1), 5–19,
 496 doi:10.15356/2076-6734-2016-1-5-19, 2016 (In Russian with English summary).
 497 Tsushima A., Matoba S., Shiraiwa T., Okamoto S., Sasaki H., Solie D.J., Yoshikawa K.: Reconstruction of recent climate
 498 change in Alaska from the Aurora Peak ice core, central Alaska, *Clim. Past*, 11, 217–226, doi:10.5194/cp-11-217-2015,
 499 2015.
 500 Vladimirova D.O. and Ekaykin A.A.: Climatic variability in Davis Sea sector (East Antarctica) over the past 250 years based
 501 on the 105 km ice core geochemical data, *Problemy Arktiki i Antarktiki*, 1 (99), 102–113, 2014. (In Russian with English
 502 summary).
 503 Volodicheva, N.: The Caucasus, in: *The Physical geography of Northern Eurasia*, edited by: Shahgedanova, M., Oxford
 504 University Press, Oxford, 350–376, 2002
 505 Wagenbach, D., Bohleber, P. and Preunkert, S.: Cold alpine ice bodies revisited: what may we learn from their impurity and
 506 isotope content? *Geografiska Annaler: Series A, Physical Geography*, 94, 245–263. doi:10.1111/j.1468-0459.2012.00461.x,
 507 2012.



510
511
512 Fig. 1: Map showing the region around Elbrus (black rectangle in the world's map in the lower right corner), with shading
513 indicating elevation (m above sea level). Drilling sites are indicated with red filled circles, GNIP stations as green filled circles, and
514 meteorological stations as blue dots. Stations situated to the south of the Main Caucasus Ridge according to the precipitation cycle
515 pattern are shown using a blue dot with white outside circle and the stations situated to the north are displayed with black outside
516 circle (see text for the details). The number of the various stations refers to Table 1 for their detailed description.
517
518

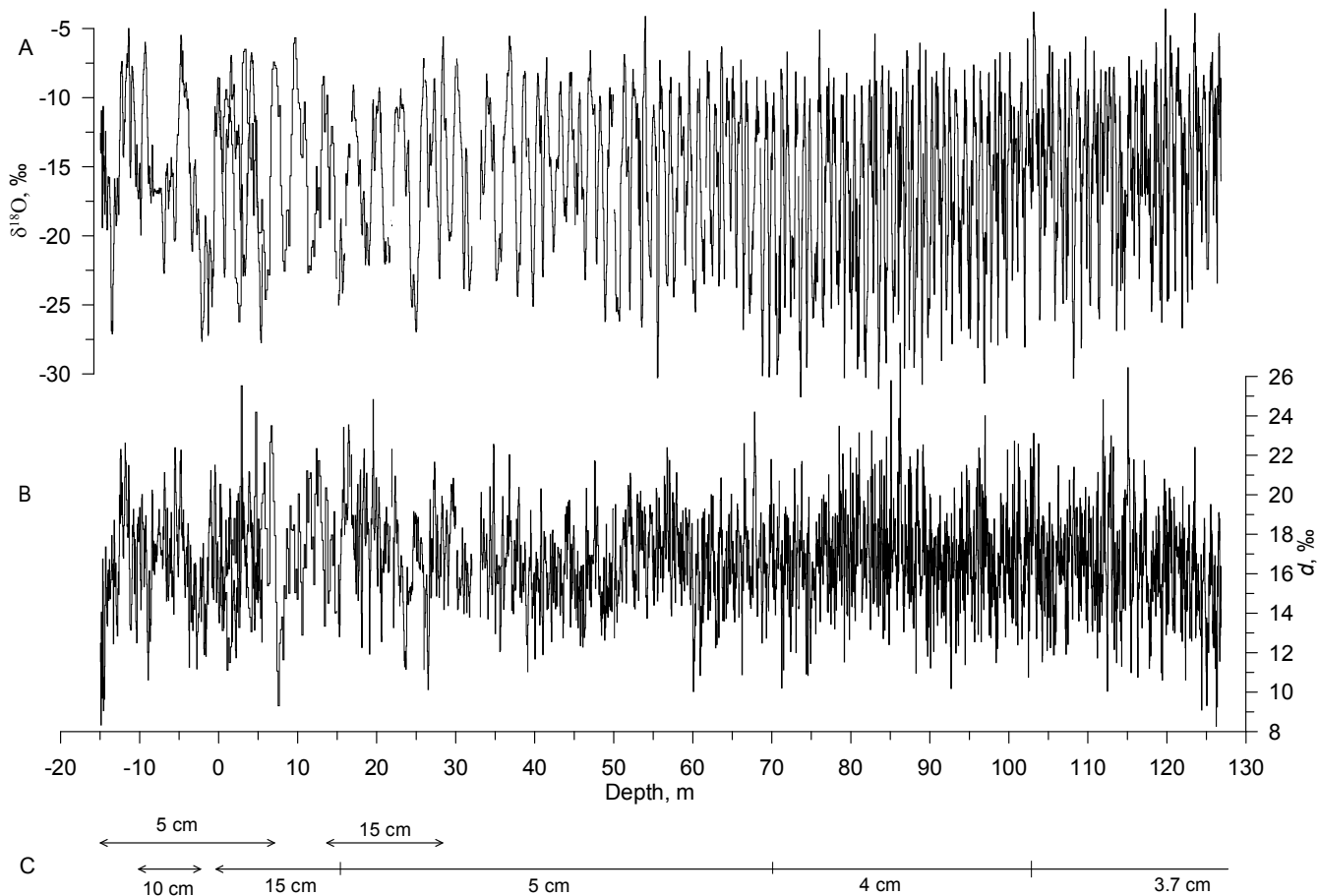


Fig. 2. Vertical profile of $\delta^{18}\text{O}$ (A), deuterium excess (B), and the number of the ice core as well as sampling resolution (C). 0 m depth corresponds to the surface of 2009.

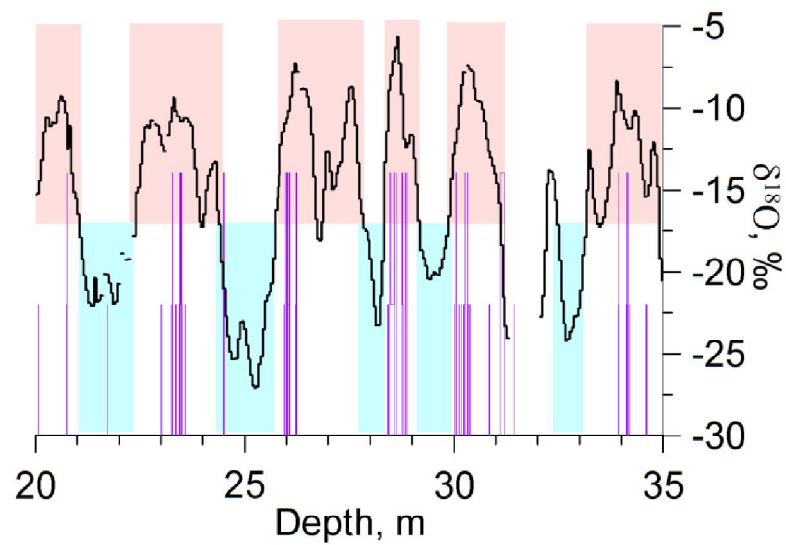


Fig. 3: Illustration of the scheme used to identify warm and cold half-years (respectively indicated by the light red and light blue shaded areas) based on the deviation of the mean $\delta^{18}\text{O}$ values from the long-term average value. The purple lines depict the melt layers observed in the core.

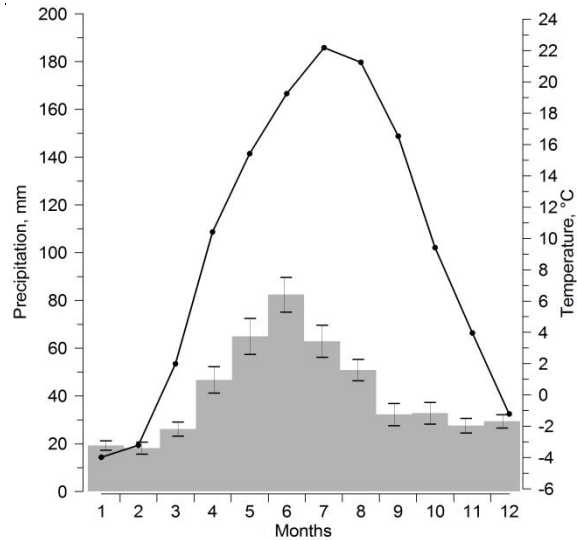
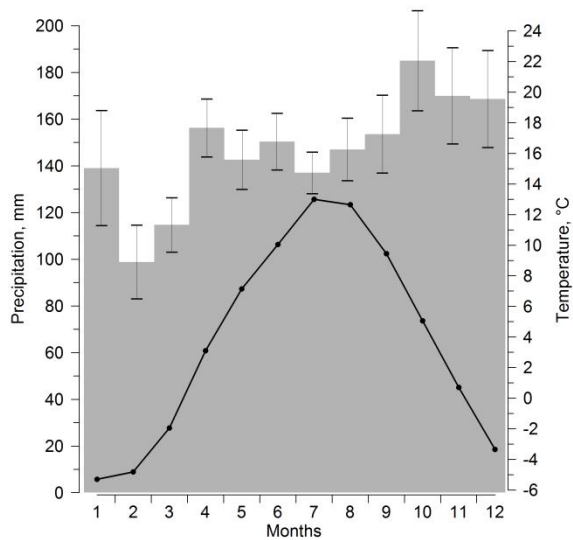


Fig. 4: Average seasonal cycle of temperature (black dots and line) and precipitation (grey bars) calculated over 1966-1990 period, a) for the Klukhorsky Pereval station (illustrating the lack of a distinct seasonal cycle in precipitation south of the Caucasus) and b) for the Mineralnye Vody station (illustrating the clear seasonal cycle in precipitation seen in stations north of the Caucasus). Error bars (SEM) are shown for the interannual standard deviation of the monthly precipitation rate while the same error bars for the temperature are dimensionless at the scale of the graph.

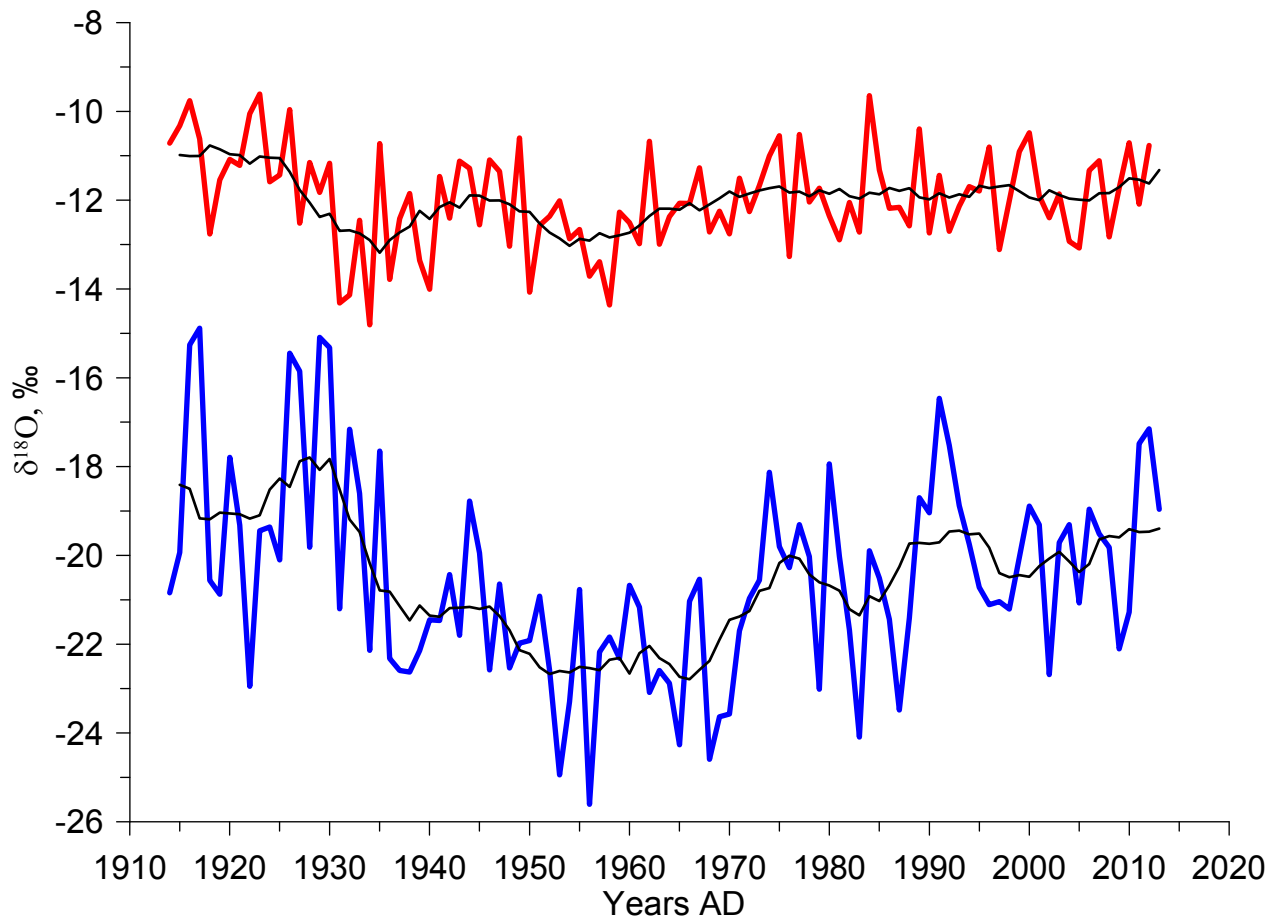


Fig. 5: Annual variations of $\delta^{18}\text{O}$ in summer (red line) and in winter (blue line). Thin black lines show 10-year running means of these parameters.

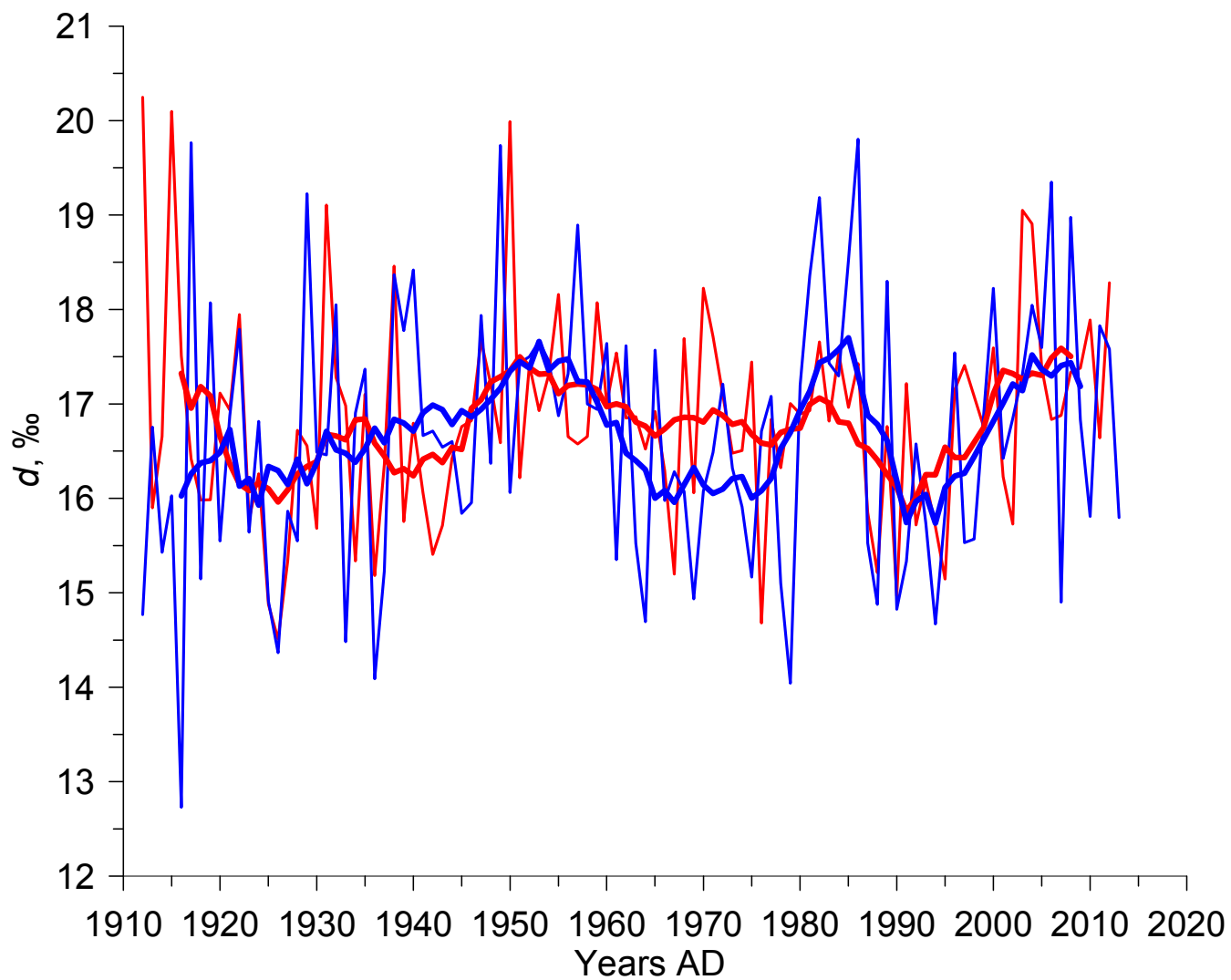


Fig. 6: Annual variations of deuterium excess in summer (red line) and in winter (blue line). Thick lines show the 10-year smoothed values and the thin ones display the raw values.

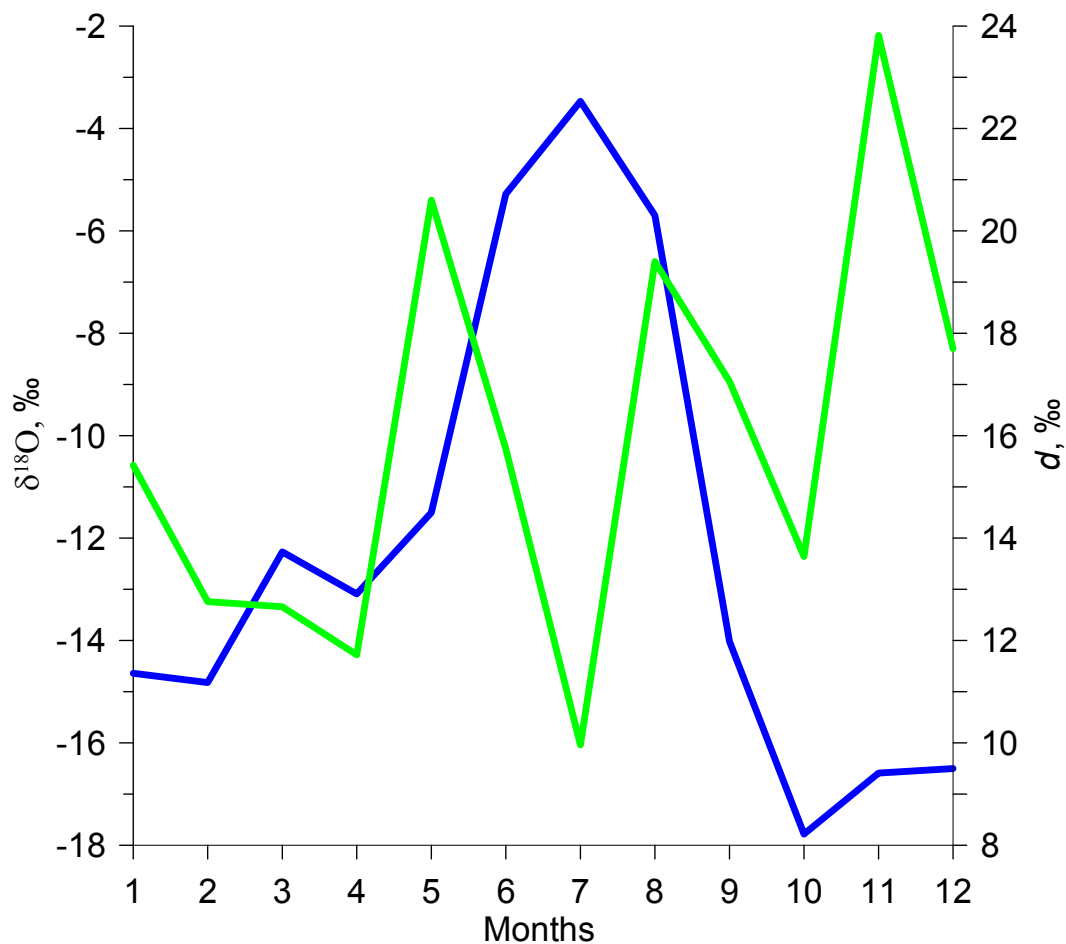


Fig. 7: Monthly $\delta^{18}\text{O}$ (blue line) and d (green line) data at Bakuriani GNIP station in 2009 (see Table 1 for information on station and Fig. 1 for its location). Note that there is no clear seasonal cycle in deuterium excess, in contrast with $\delta^{18}\text{O}$ showing maximum values in summer and minimum values in winter.

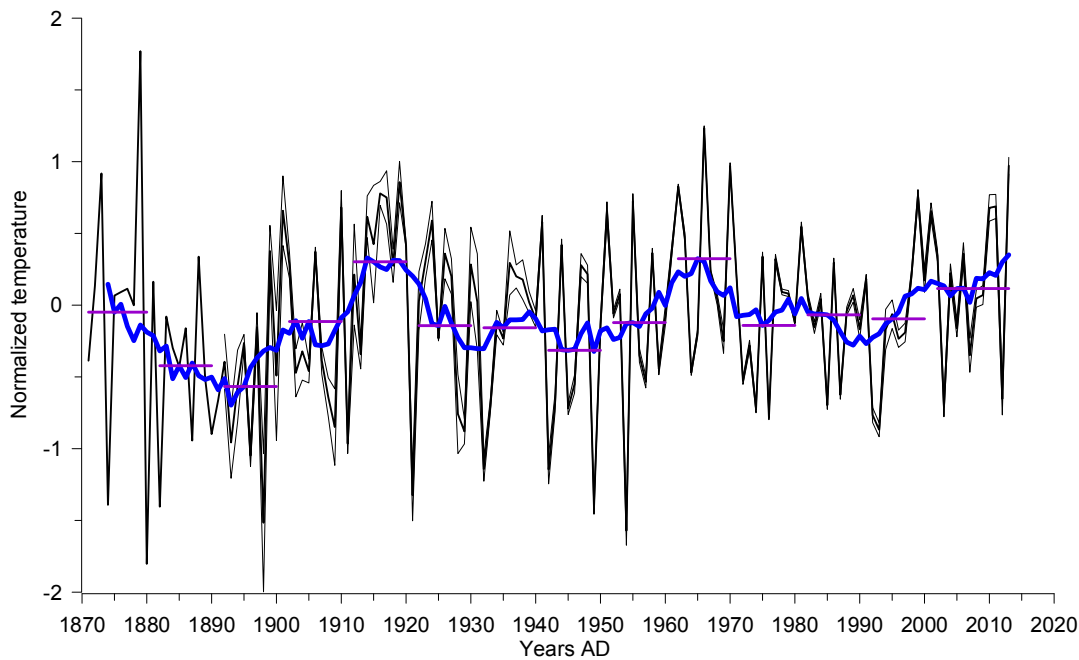
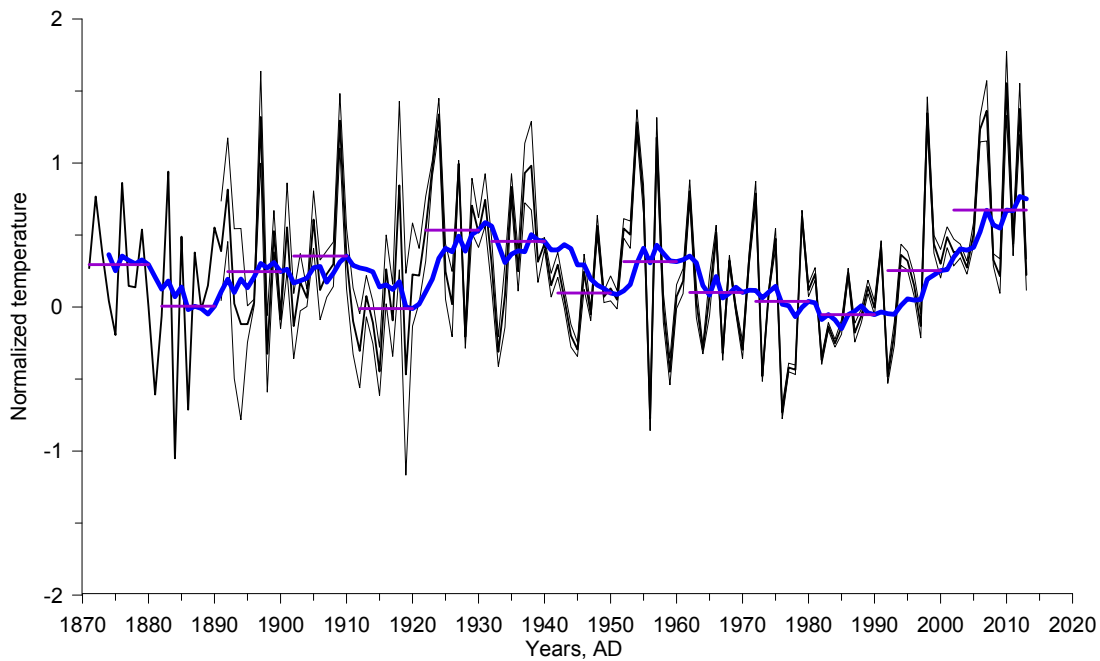


Fig. 8: Normalized regional temperature record based on meteorological data, with respect to the reference period 1966-1990, expressed as annual anomalies ($^{\circ}\text{C}$). The thin lines illustrate the standard deviation across the individual records after accounting for the lapse rate from Fig. S3, the blue line shows 10 year running mean and the horizontal purple line demonstrates the decadal mean value, the upper panel for the warm season, and the lower panel for the cold season.

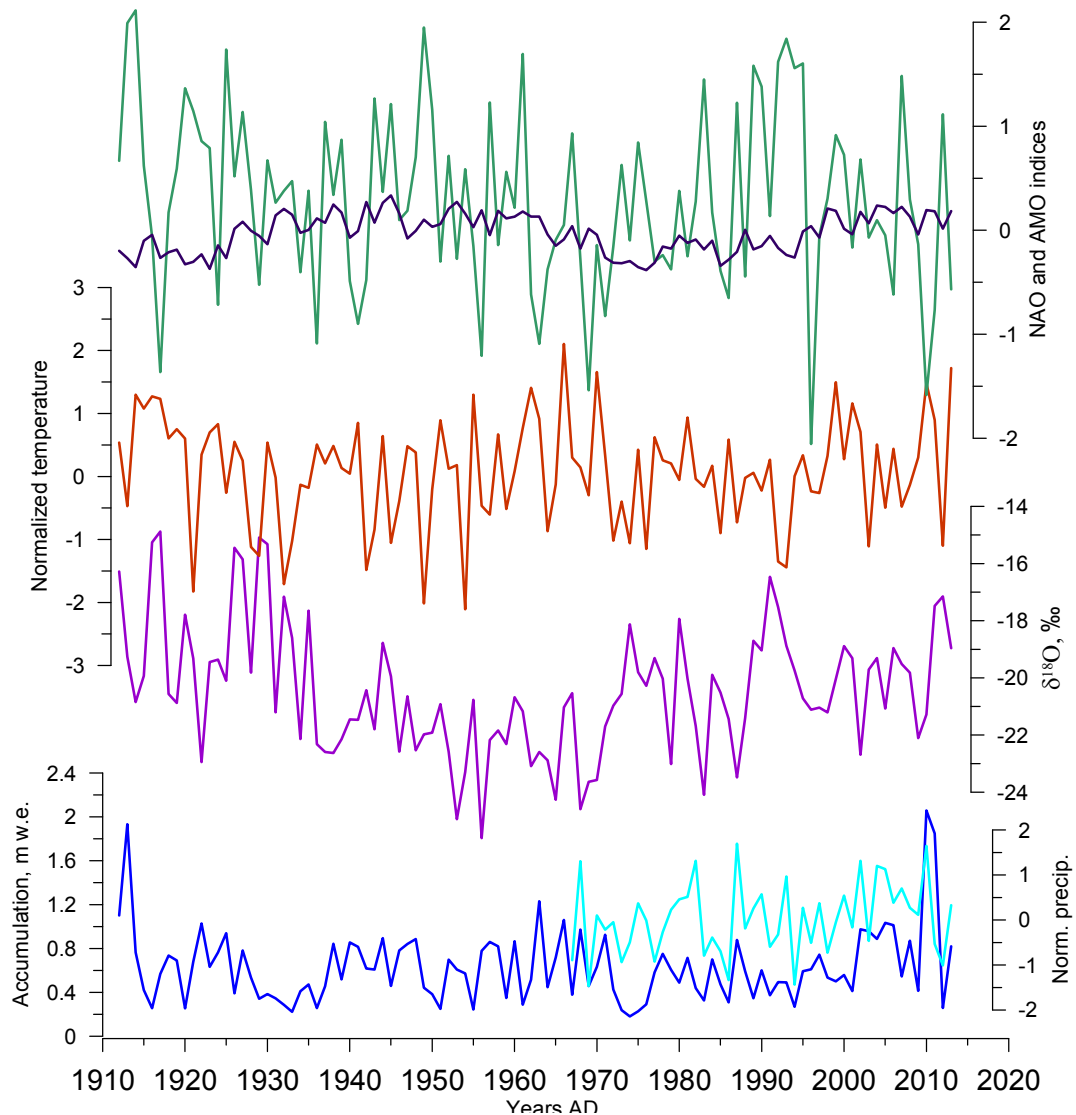


Fig. 9: Comparison of the ice core record with instrumental regional climate information, for the cold season: $\delta^{18}\text{O}$ composite (purple), regional meteorological composites of temperature (brown), precipitation to the south from the Caucasus (light blue) as well as the ice core accumulation estimate (dark blue) and NAO (green) and AMO (dark) indices.

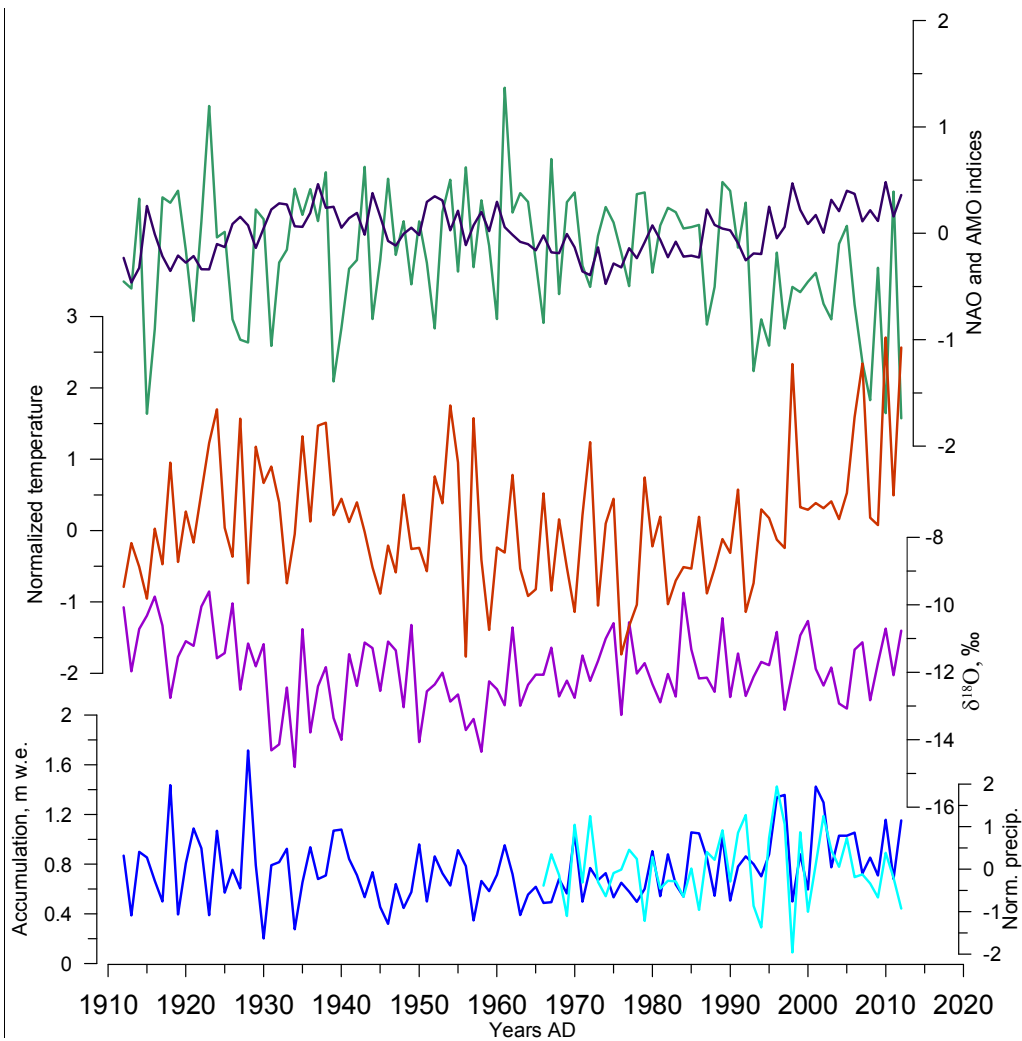


Fig. 10: Comparison of the ice core record with instrumental regional climate information, for the warm season: $\delta^{18}\text{O}$ composite (purple), regional meteorological composites of temperature (brown), precipitation to the south from the Caucasus (light blue) as well as the ice core accumulation estimate (dark blue) and NAO (green) and AMO (dark) indices.

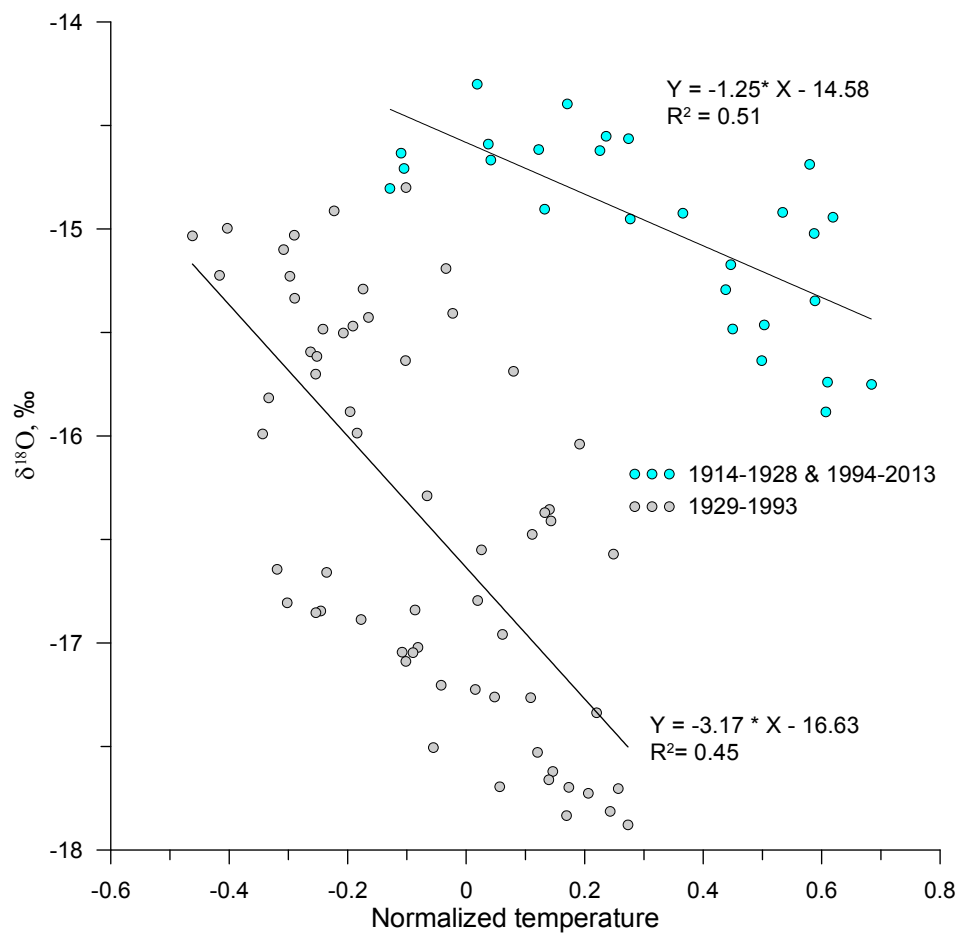


Fig. 11. Correlation plot and regression lines for the 11-year running means of the annual local temperature and annual $\delta^{18}\text{O}$.

Data type	Number on map (Fig. 1)	Location/Name	Altitude a.s.l.	Time span	Data source
Meteorological observations (temperature, precipitation rate) with daily resolution	1	Sochi	57 m	1871-present	www.meteo.ru
	2	Mineralnye Vody	315 m	1938-present	
	3	Kislovodsk	943 m	1940-present	
	4	Pyatigorsk	538 m	1891-1997	
	5	Shadzhatmaz	2070 m	1959-present	
	6	Terskol	2133 m	1951-2005	
	7	Klukhorskiy Pereval	2037 m	1959-present	
	8	Teberda	1550 m	1956-2005	
	9	Sukhumi	75 m	1904-1988	
	10	Samtredia	24 m	1936-1992	
	13	Tbilisi	448 m	1881-1992	
	14	Sulak	2927 m	1930-present	
	15	Mestia	1417 m	1930-1991	
GNIP data	11	Batumi	32 m	1980-1990	http://www-naweb.iaea.org/napc/ih/IHS_resources_gnip.html
	12	Bakuriani	1700 m	2008-2009	
	13	Tbilisi	448 m	2008-2009	
Circulation indices	n/a	NAO	n/a	1821-present	Vinter et al., 2009 https://crudata.uea.ac.uk/~timo/datasets/naoi.htm
			n/a	1950-present	http://www.cpc.ncep.noaa.gov/products/precip/CWlink/
	n/a	NCP	n/a	1948-present	
	n/a	AO	n/a	1950-present	
	n/a	AMO	n/a	1856-present	
Reanalysis daily temperature	n/a	NCEP	500 mb level	1948-present	http://www.esrl.noaa.gov/psd/data/gridded/data.ncep.reanalysis.html Kalnay et al., 1996
Back trajectories	n/a	Flexpart	n/a	2002-2009	Forster et al., 2007, Stohl et al., 2009
	n/a	Hysplit	n/a	1948-present	Draxler, 1999, Stein et al., 2015, Rolph, 2016
	n/a	LMDZiso	n/a	n/a	Risi et al., 2010

578

579

580

Table 2: Correlation coefficients between meteorological data and indices of large-scale modes of variability (statistically significant coefficients at $p < 0.05$ are highlighted in bold).

	SUMMER			WINTER		
	Temperature	P south*	P north*	Temperature	P south*	P north*
NAO	-0.47	0.23	-0.03	-0.41	0.04	0.26
AO	-0.11	0.08	-0.14	-0.40	0.14	0.37
AMO	0.24	0.01	-0.02	0.07	0.27	0.25
NCP	-0.50	0.34	0.18	-0.77	0.25	0.33

581

582

583

584

*P south – precipitation rate at the weather stations to the South from the Caucasus, P north – precipitation rate at the weather stations to the North from the Caucasus.

585
586

Table 3: Mean characteristics of the Elbrus ice core records, calculated for the period from 1914 to 2013.

Winter	$\delta^{18}\text{O}$, ‰	δD , ‰	d , ‰	Accumulation rate (mm w.e./year)
Mean	-21.20	-152.42	17.16	0.61
Standard deviation	2.18	17.44	1.41	0.31
Summer				
Mean	-11.80	-77.32	17.06	0.76
Standard deviation	1.02	8.10	1.15	0.26

587
588

589
590
591

Table 4. Correlation coefficients between ice core data, meteorological data and indices of large-scale modes of variability (statistically significant coefficients at $p < 0.05$ are highlighted in bold).

Summer	$\delta^{18}\text{O}$	Accumulation	d	NAO	AO	NCP
T . °C	0.13	0.09	0.21	-0.48	-0.10	-0.51
P north	0.07	0.24	0.11	-0.03	-0.14	0.18
P south	-0.12	0.44	-0.04	0.23	0.08	0.34
$\delta^{18}\text{O}$		-0.17	-0.11	0.06	0.23	-0.04
Accumulation			0.27	-0.25	0.05	0.07
d				-0.17	0.00	-0.18
Winter	$\delta^{18}\text{O}$	Accumulation	d	NAO	AO	NCP
T . °C	-0.02	0.31	-0.08	-0.42	-0.45	-0.79
P north	0.25	0.13	-0.01	0.26	0.37	0.23
P south	-0.09	0.44	-0.06	0.04	0.14	0.25
$\delta^{18}\text{O}$		-0.05	-0.04	0.42	0.34	0.08
Accumulation			0.04	-0.34	-0.35	0.05
d				0.05	-0.09	0.04

592
593

*P south – precipitation rate at the weather stations to the South from the Caucasus, P north – precipitation rate at the weather stations to the North from the Caucasus.